



City Research Online

## City, University of London Institutional Repository

---

**Citation:** Yan, D., Kovacevic, A. & Tang, Q. (2017). Numerical investigation of cavitation in twin-screw pumps. *Proceedings of the Institution of Mechanical Engineers, Part C: Journal of Mechanical Engineering Science*, 232(20), pp. 3733-3750. doi: 10.1177/0954406217740927

This is the accepted version of the paper.

This version of the publication may differ from the final published version.

---

**Permanent repository link:** <https://openaccess.city.ac.uk/id/eprint/19907/>

**Link to published version:** <https://doi.org/10.1177/0954406217740927>

**Copyright:** City Research Online aims to make research outputs of City, University of London available to a wider audience. Copyright and Moral Rights remain with the author(s) and/or copyright holders. URLs from City Research Online may be freely distributed and linked to.

**Reuse:** Copies of full items can be used for personal research or study, educational, or not-for-profit purposes without prior permission or charge. Provided that the authors, title and full bibliographic details are credited, a hyperlink and/or URL is given for the original metadata page and the content is not changed in any way.

---

City Research Online:

<http://openaccess.city.ac.uk/>

[publications@city.ac.uk](mailto:publications@city.ac.uk)

---

# Numerical Investigation of Cavitation in Twin-screw Pump

Di Yan<sup>1,2</sup>, Ahmed Kovacevic<sup>2</sup>, Qian Tang<sup>1</sup>, Sham Rane<sup>2</sup>

<sup>1</sup>State Key Laboratory of Mechanical Transmission, Chongqing University, 400044, China;

<sup>2</sup>Centre for Compressor Technology, City University London, EC1V0HB, UK

## Abstract

In order to investigate the flow characteristics and the formation process of cavitation in twin-screw pumps, three-dimensional CFD (Computational Fluid Dynamics) numerical analysis has been carried out. A conformal structured moving mesh generated by an in-house code SCORG was applied for the rotor domain. The VOF (Volume of Fluid) Method has been adopted for dealing with the liquid-gas two-phase flow, while the bubble dynamics was handled by a homogenous cavitation model. By changing the rotation speed and discharge pressure, the intensity, distribution area and variation of cavitation at different rotor angle were obtained. The effects of rotation speed and discharge pressure on cavitation characteristics have been analysed. Calculation results with cavitation model are compared with the results without cavitation and the experimentally obtained values. The influence of cavitation on the performance of a screw pump in terms of the mass flow rate, pressure distribution, rotor torque and the shaft power have been analysed and discussed. For analysis of cavitation in clearances, a 2-D numerical model which includes radial and inter-lobe clearances was used. The relationship between volumetric efficiency and cavitation intensity was developed by variation of boundary conditions.

**Keywords:** Screw Pump, Cavitation, Moving Mesh, CFD, Numerical Modelling, Cavitation in Clearances

## 1. Introduction

Twin screw pumps are positive displacement machines widely used in petrochemical, shipping, energy and food industries due to their reliability, self-priming capability and excellent performance in single phase or multiphase operation. Typical arrangement of a twin screw liquid pump is given in Figure 1, showing rotors synchronised by timing gears and enclosed in the casing.

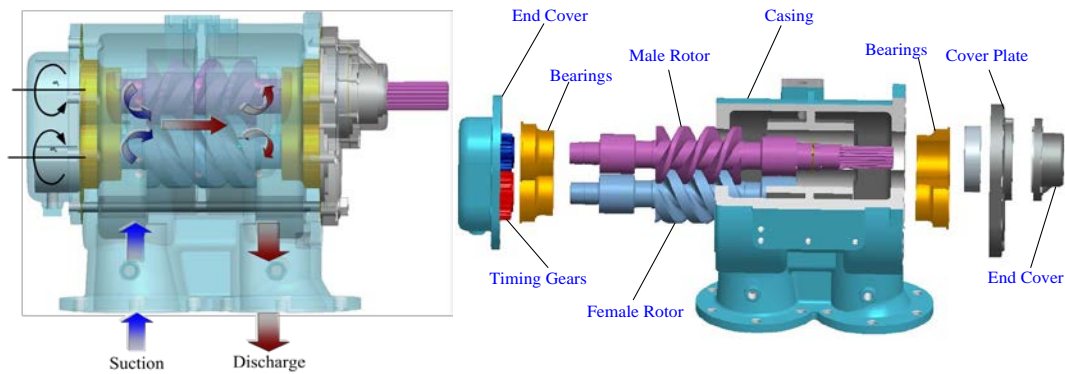


Figure 1 Structure and components of twin-screw pump

With the trend of increasing rotational speed, delivery pressure and power in screw pumps, the cavitation becomes a phenomenon unavoidable in such kinds of machines. Nowadays, the research of cavitation is mainly focused on centrifugal pumps, hydrofoils, propellers and hydraulic valves, etc. (Figure 2)[1]. The lobes of a positive displacement screw pump are much thicker than in turbo machines, while the clearances of screw pumps are much smaller than in dynamic pumps. Positive displacement machines also rotate slower than equivalent size dynamic machines. Therefore such machines are less sensitive to cavitation, and usually no obvious cavitation erosion is observed on screw rotor surfaces. For that reason less attention is paid in the literature to the cavitation in screw pumps [2]. However, during the rotation of screw rotors, cavitation develops through initiation, growth and collapse of bubbles, which will directly influence the performance of a screw pump, such as increasing vibration and noise, eroding surfaces of rotors and casing wall, lowering the volumetric efficiency, and so on [3]. Therefore, in order to improve the performance and stability of screw pump and expand its application fields, cavitation cannot be ignored.

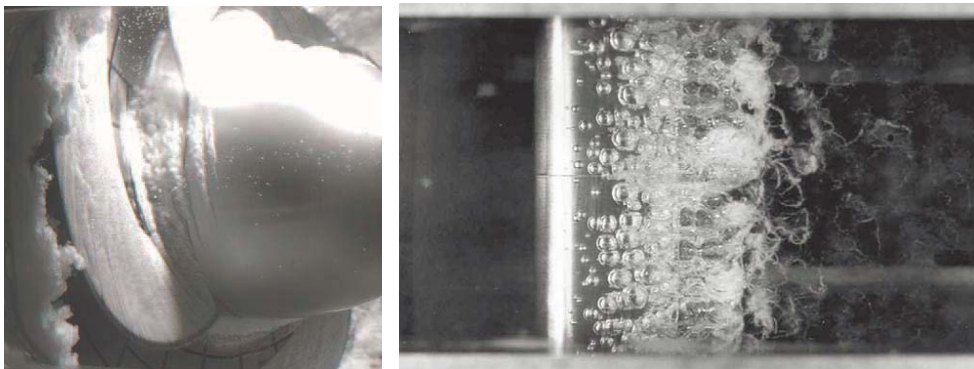


Figure 2 Cavitating flow in the inducer of a turbo pump (left); Hydrofoil (right) [1]

Increasing demands for high-performance screw pumps require improvements in pump designs. But for improvements in the design of screw pumps, full understanding of process within the pump is indispensable. Research work on modelling and experimental investigation of working processes in twin screw pumps was reported in many previous studies. The number of literature resources is large and therefore just the most relevant will be listed below.

O.A. ПЫЖ etc. [4] elaborated the rotor profile generation and performance analysis of four typical marine screw pumps. Li [5] introduced the structure, rotor profiles generation and performance calculation of different kinds of screw pumps. Feng Cao et al. [6] proposed

calculation models for the back flow and pressure generation within the multiphase twin-screw pump and also simulated the thermodynamic performance and the transport behaviour of the pump with different gas volume fractions. Tang and Zhang [7] modelled the screw pump by use of CFD static mesh and proposed improvements to a leakage model for twin-screw pump. In addition they optimised some rotor profiles. Jing Wei [8] discussed the rotor profile design of twin-screw kneader and simulated the flow field based on CFD by static grid. D. Mewes [9] proposed a performance calculation model for a multiphase pump according to the mass and energy conservation in the pump chamber and validated it by experiments. Abhay Patil [10] and Evan Chan [11] studied the steady state and transient properties under different working conditions. They discussed about the influence of the viscosity of the sealing liquid and gas void fraction on the performance of a two-phase screw pump. K. Rabiger [12] proposed a theoretical model for screw pump and carried out the numerical and experimental analysis of the performance of the pump under very high gas volume fractions (90%-99%). He also conducted an experiment to visualize the leakage flow in radial clearances.

The literature resources referenced above provide a good understanding of the working process. However, to date, most of the current methods are based on the thermodynamic chamber mathematical models which neglect kinetic energy and simplify the analysis of the main and leakage flows [13][14]. Chamber models can predict integral performance of screw pumps relatively accurately but are not taking into account 3D effects within the working domains, which means chamber models are incapable of simulating cavitation as a phenomena highly related to the geometry of flow fields. Few others refer to a steady state computational fluid dynamics (CFD) which assumes static mesh of the moving flow domains. By using static mesh, approximate pressure gradients and the leakage velocity field can be obtained; however such results do not take into account the velocity field of the main flow and neglect the transient nature of the working process in a screw pump. In addition the pressure flow losses could not be calculated. Therefore phenomena such as power losses, effect of change in clearances and any dynamic behaviour including cavitation and multiphase flows could not be analysed using such static mesh.

Breakthrough in using CFD for analysis of positive displacement screw machines was made by Kovacevic [15] who generated structured moving mesh for screw compressor rotor based on a rack generation method proposed by Stosic [16]. This pioneering work in grid generation for screw machines allowed for the CFD simulation and performance prediction of screw compressors [17]. This method provided a powerful basis for research of screw pumps. It also makes modelling of cavitation in twin-screw pump possible.

Cavitation is a very common physical phenomena which happens in almost all fluid machinery and hydraulic devices which use liquid as working medium [3]. However, it is still not understood fully to allow step change in application of such machines. Normally, the cavitation in fluid machinery is caused by local pressure drop. The occurrence of bubbles is usually because of two reasons. The first one is vaporisation of liquid when the pressure reaches its saturated vapour pressure. The other is the gas dissolved in liquid which is released by occurrence of low pressure. For example, in water and oil pumps air can often be dissolved in the liquid. However, the formation mechanism of cavitation and its influence factors are difficult to be precisely captured and described. For example, in a liquid pump, the formation and distribution of cavitation can be easily influenced by fluid property, suction and discharge

pressure, temperature, rotation speed, chamber geometry, clearances and etc [18].

When the working fluid is water, the bubbles mainly come from vapour. But for many hydraulic machinery and equipment, the working fluid is usually mineral oil. By experimental investigation [19], it was found that the saturated vapour pressure of oil is far below that of water at normal temperatures. Therefore bubbles which come from vaporised oil are unlikely to appear and can be neglected. Instead, the bubbles are mainly initiated from nuclei of non-condensable gas dissolved in oil.

The research of cavitation is mainly carried out by experimental and numerical methods. By numerical simulation based on cavitation model, the area and location of bubbles can be predicted [20], and then validated by comparison with experimental observation through high-speed photography [21], particle image velocimetry (PIV), etc. However, there are considerable limitations for experimental methods. Firstly they are costly and usually suitable for simple flow fields such as venturi tube or nozzle orifice. For high-speed and non-transparent fluid flow and complex geometry, it is difficult to observe and investigate cavitation by experiment. Accordingly, numerical methods are still the main tool to study the cavitation in majority of fluid machines. They are based on simplified cavitation models that have been validated by mathematical and experimental studies to have sufficient accuracy for relatively simple cases they were applied to.

With the increasing developments of computing technology and numerical methods, nowadays many cavitation models are proposed. Such as Singhal full cavitation model [22], Zwart model [23], Kunz model [24] and Sauer-Scherr model [25][26][27]. Integrated within commercial solvers, these models are widely used in analysis of centrifugal pumps, turbines, hydraulic valves, hydrofoils and so on. They are relatively efficient and accurate. For example, Mireia Altimira and Laszlo Fuchs [28] investigated throttle flow under cavitating conditions based on Sauer-Scherr model and VOF method by using the implicit LES (Large Eddy Simulation) approach and they also validated the results by experiment. Desheng Zhang, et al. [29] simulated and analysed 3-D tip leakage vortex cavitation and the suction-side-perpendicular cavitating vortices in an axial pump by applying Zwart model and an improved SST  $k-\omega$  turbulence model, the simulation results matched well with high speed photography results. Since many cavitation models are embedded with commercial solvers, it becomes convenient and efficient to model cavitation for fluid machinery, as was stated above.

Till now, no reference was found on investigation of cavitation in twin-screw pumps. Yet, there are some analysis cases for positive displacement pumps. For example, Yingyuan Liu, et al. [30] applied Zwart model in cavitation analysis of rotor pumps based on 2-D unstructured moving mesh, the influences of rotation speed, pressure difference, clearance size and inlet pressure on cavitation were investigated. David del Campo, et al. [18][31] investigated cavitation in external gear pumps by using Zwart model and observed the chamber flow field by Time-Resolved Particle Image Velocimetry (TRPIV), the inlet and outlet pressure effects were discussed. A. King et al. [32] combined one-dimensional and three-dimensional CFD models to improve the design of a gear pump porting and reduce cavitation erosion. The cases above can be referenced for screw pump analysis.

In this paper, the unique grid generation software SCORG developed by authors is used for grid generation of a structured moving mesh around screw pump rotors [33]. The mesh for stationary domains such as ports and pipes is generated by use of a commercial grid generator built into

the CCM (Computational Continuum Mechanics) solver STAR-CCM+ [34]. Handling of the mesh generated by SCORG in STAR-CCM+ solver is managed by use of the UDF made specially for handling conformal rotor mesh and it will be described later in the paper. This method has been validated by experiment in single-phase CFD modelling of screw pump [35][36].

This paper is aimed to study the flow characteristics of twin-screw pumps under cavitating conditions. Based on the structured moving mesh, full CFD simulations with and without cavitation have been carried out and will be explained in detail in this paper. The real-time mass flow rate, rotor torque, pressure distribution, velocity field, power consumption were obtained. In cavitation modelling, Volume of Fluid (VOF) model [37] was applied for dealing with the liquid-gas two-phase flow. The Sauer-Schnerr model was used for modelling bubble dynamics. By changing rotation speed and discharge pressure separately, the accordingly variation of cavitation was acquired. The influence of cavitation on performance of a screw pump and the mechanism of cavitation in clearances were analysed and discussed.

## 2. Mathematical Model

Positive displacement screw pumps operate on the basis of changing the size and position of a working domain which consequently causes change in the pressure of the working domain thereby transporting the fluid. To calculate performance of a screw pump, quantities such as mass, momentum, energy etc. need to be modelled.

The governing equations required for the solution a closely coupled, time dependent set of partial differential equations (PDE's) and often employ a Finite Volume Method (FVM) to be solved [38][39].

### 2.1 Governing Equations

The cavitating flow can be treated as a homogeneous mixture of vapour, air and liquid, in which vapour and air are gas. So it is liquid-gas two-phase flow.

VOF considers a single effective fluid whose properties vary according to volume fraction of individual fluids:

$$\alpha_i = \frac{V_i}{V} \quad (1)$$

The mass conservation equation for fluid  $i$  reads:

$$\frac{\partial(\alpha_i \rho_i)}{\partial t} + \nabla \cdot (\alpha_i \rho_i \mathbf{v}) = \rho_i S_{\alpha_i} \quad (2)$$

It can be rearranged into an equation in integral form:

$$\frac{\partial}{\partial t} \int_V \alpha_i dV + \int_S \alpha_i \mathbf{v} \cdot \mathbf{n} dS = \int_V \left( S_{\alpha_i} - \frac{\alpha_i D_{\rho_i}}{\rho_i Dt} \right) dV \quad (3)$$

where  $S_{\alpha_i}$  is the source of the phase  $i$

This equation is used to compute the transport of volume fraction  $\alpha_i$

The mass conservation equation for the effective fluid is obtained by summing up all

component equations and using the condition:

$$\sum_i \alpha_i = 1 \quad (4)$$

The integral form of mass conservation equation (used to compute pressure correction) reads:

$$\int_S \mathbf{v} \cdot \mathbf{n} dS = \sum_i \int_V \left( S_{\alpha_i} - \frac{\alpha_i D\rho_i}{\rho_i Dt} \right) dV \quad (5)$$

The properties of effective fluid are computed according to volume fractions:

$$\rho = \sum_i \alpha_i \rho_i \quad (6)$$

The VOF model description assumes that all immiscible fluid phases present in a control volume share velocity, pressure, and temperature fields. Therefore, the same set of basic governing equations describing momentum, mass, and energy transport as in a single-phase flow is solved.

The equations are solved for an equivalent fluid whose physical properties are calculated as functions of the physical properties of its constituent phases and their volume fractions.

## 2.2 Cavitation Model

The cavitation model describes the growth of bubbles which includes the phase change between liquid and its vapour. In this calculation, a homogenous distribution of bubble seeds in the liquid was applied. Based on the Rayleigh-Plesset equation [40], the vapour volume fraction can be calculated as follows:

$$\alpha_v = \frac{V_v}{V_l + V_v} = \frac{n_0 V_l \frac{4}{3} \pi R^3}{V_l + n_0 V_l \frac{4}{3} \pi R^3} = \frac{n_0 \frac{4}{3} \pi R^3}{1 + n_0 \frac{4}{3} \pi R^3} \quad (7)$$

The bubble growth rate can be described as:

$$\dot{R} = \frac{dR}{dt} = \sqrt{\frac{2 P_B - P_\infty}{3 \rho_l}} \quad (8)$$

then the vapour production rate can be calculated as follows:

$$\frac{d\alpha}{dt} = (1 - \alpha) \frac{4\pi n_0 R^2}{1 + \frac{4}{3} n_0 \pi R^3} \dot{R} \quad (9)$$

The continuity equation can be written as follows:

$$\nabla \cdot \mathbf{v} = -\frac{1}{\rho} \left( \frac{\partial \rho}{\partial t} + \mathbf{v} \cdot \nabla \rho \right) = -\frac{1}{\rho} \frac{d\rho}{dt} = \frac{\rho_l - \rho_v}{\rho} \frac{d\alpha}{dt} \quad (10)$$

Then the following transport equation can be derived.

$$\frac{d\alpha}{dt} + \nabla \cdot (\alpha \mathbf{v}) = \frac{d\alpha}{dt} + \alpha \nabla \cdot \mathbf{v} = \frac{(1 - \alpha) \rho_l}{(1 - \alpha) \rho_l + \alpha \rho_v} \frac{n_0}{1 + n_0 \frac{4}{3} \pi R^3} \frac{d}{dt} \left( \frac{4}{3} \pi R^3 \right) \quad (11)$$

### 3. Setup for Calculation of the Screw Pump

The screw pump used for this study shown in Figure 1 is a twin-screw pump with a 2/3 lobe arrangement and A-type profile rotors. The operating speed of the male rotor changes from 630 to 2100 rpm while keeping the discharge pressure as 0.85 MPa. By controlling the discharge valve, the discharge pressure varies from 0.35 to 0.85 MPa while keeping rotation speed of the male rotor at 2100 rpm. The male and the female rotors have 140.00 mm diameter and the centre distance of 105.00 mm. The length of the rotors is 200.00 mm and the male rotor has a wrap angle of 590.0°.

#### 3.1 Grid Generation

Grid generation is a process of discretising a working domain of the screw pump in control volumes for which a solution of local fluid properties is to be found. It may be numerical, analytical or variational [41]. The results obtained in this research work used grids generated by analytical grid generation. Applying the principles of analytical grid generation through transfinite interpolation with adaptive meshing, the authors have derived a general, fast and reliable algorithm for automatic numerical mapping of arbitrary twin screw machine geometry built into an in-house grid generation code SCORG [17].

The rotor profile of the screw pump is shown in Figure 3. Table 1 shows the geometry parameters of rotors. The numerical grid for the working fluid domain between two rotors is shown as Figure 4. Configuration of the mesh around rotors is given by Table 2.

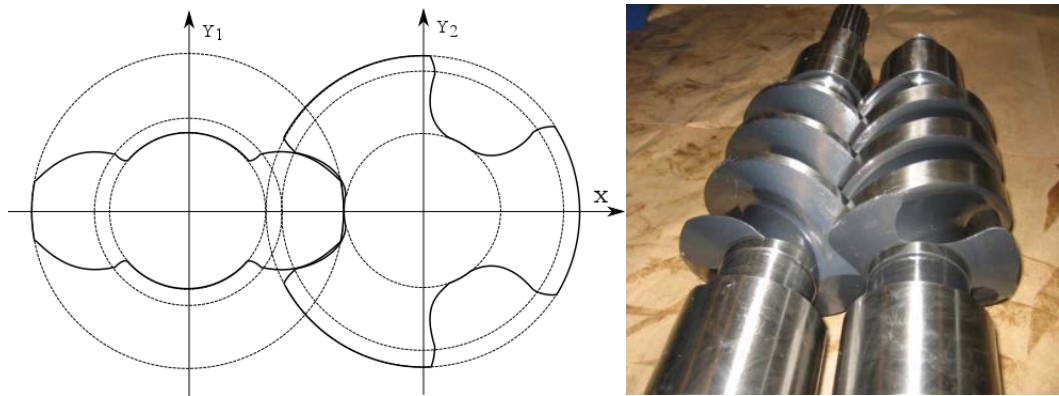


Figure 3 A-type tooth profile used in this paper

Table 1 Geometry parameters of screw rotors used in study

	Number of Lobes	Pitch Radius (mm)	Root Radius (mm)	Tip Radius (mm)
Male Rotor	2	42	35	70
Female Rotor	3	63	35	70
Centre distance		105mm		
Thread pitch		61mm		
Radial clearance		0.24mm		
Inter-lobe clearance		0.12mm		

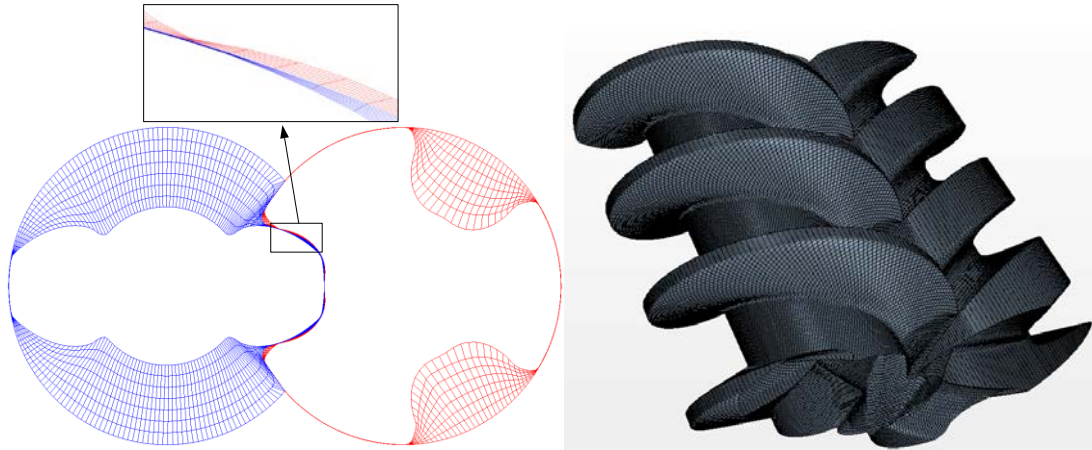


Figure 4 Grids in the fluid domain around rotors  
a) in cross section of rotors b) on the rotor surface

Table 2 Mesh configuration of fluid domains around rotors

Circumferential divisions	75
Radial divisions	7
Axial divisions	75
Interface divisions	78
Number of profile points	1000

Polyhedral mesh of the inlet port and outlet port is generated using STAR-CCM+ grid generator as shown in Figure 5. The grid independency study for this calculation model has already been performed in another publication [35].

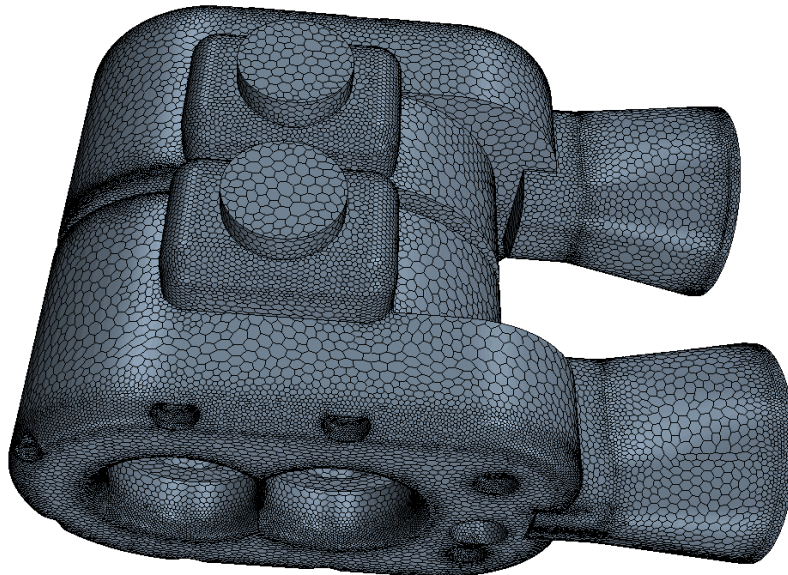


Figure 5 Polyhedral mesh of suction and discharge ports

A numerical mesh used in this study comprises 1068864 cells of which 775180 cells represent the fluid domain between the rotors while 293684 cells represent the two ports.

### 3.2 Numerical Methods

The Star-CCM+ pressure-based solver is used for the calculation of screw pump. In order to solve the pressure-velocity coupling, the implicit unsteady segregated flow scheme has been applied. The second-order upwind discretization scheme is applied. Gauss-Seidel node is used for the relaxation scheme which provides better convergence by iteratively correcting (relaxing) the linear equation during multigrid cycling.

The main rotor rotates  $2.4^\circ$  per step. The mesh is updated before commencing solution for each time step. The time-step is defined as follows:

$$\Delta t = \frac{DPTS}{6 \cdot RPM} \quad (12)$$

whereby,  $DPTS$  is the degree per time step,  $RPM$  is the rotation speed of male rotor.

When the  $DPTS$  is not small enough, it will make the simulation run with a relatively large time-step which may cause the divergence of calculation. Here,  $\Delta t$  is inversely proportional to  $RPM$ , which means that the mesh has to be changed for different  $RPM$  in order to keep the ratio of time and spatial step constant. It's not always essential to keep the ratio constant but it is limited by Courant stability condition [17].

The k- $\epsilon$  turbulence model is adopted in the calculation. Different turbulence models have been compared during this simulation, the results show that the variation in mass flowrate with difference turbulence models is less than 0.2% which is small enough for the overall performance prediction [36]. Stagnation inlet and pressure outlet are used respectively for the inlet and outlet boundaries. The pressure of the inlet port is 0 Pa. The discharge pressure ranges from 0.35 to 0.85MPa while the rotation speed of the male rotor ranges from 630 to 2100 rpm. The initial pressure and initial velocity are 0 Pa and 0 m/s respectively. The turbulence intensity is 1% and the turbulence viscosity ratio is 10.

## 4. Numerical Results

The calculations were carried out in a computer powered by 4 Intel 3.00 GHz processors and 8 GB memory. Screw pump rotation was simulated by means of 75 time steps for one interlobe rotation, which was equivalent to 150 time steps for one full rotation of the male rotor. The time step length was synchronised with a rotation speed of 630 to 2100 rpm. An error reduction of 4 orders of magnitude was required, and achieved in 30 inner iterations at each time step. The overall performance parameters such as chamber pressure, velocity distribution, rotor torque, mass flow rate and shaft power were then calculated.

### 4.1 Cavitation under Different Boundary Conditions

The start-up process of a screw pump is highly unsteady leading to the large area of cavitation in the pump chamber in a short period of time. As time progresses, the flow field gradually reaches a steady state condition when the domain in which fluid cavitates becomes reduced and repeats periodically. Figure 6 shows the maximum volume fraction of vapour observed in the working domain as the function of the rotation angle under different rotation speed and the

constant discharge pressure. It can be observed from Figure 6(up) that rotation speed effects the occurrence of cavitation. In an unsteady state, volume fraction of cavitation increased with the increase in rotation speed. A longer time is required to reach a steady state condition for higher rotation speed. From Figure 6(down) it can be observed that, when cavitation stabilized, the volume fraction of cavitation and its fluctuation amplitude repeat and are higher for higher rotation speeds.

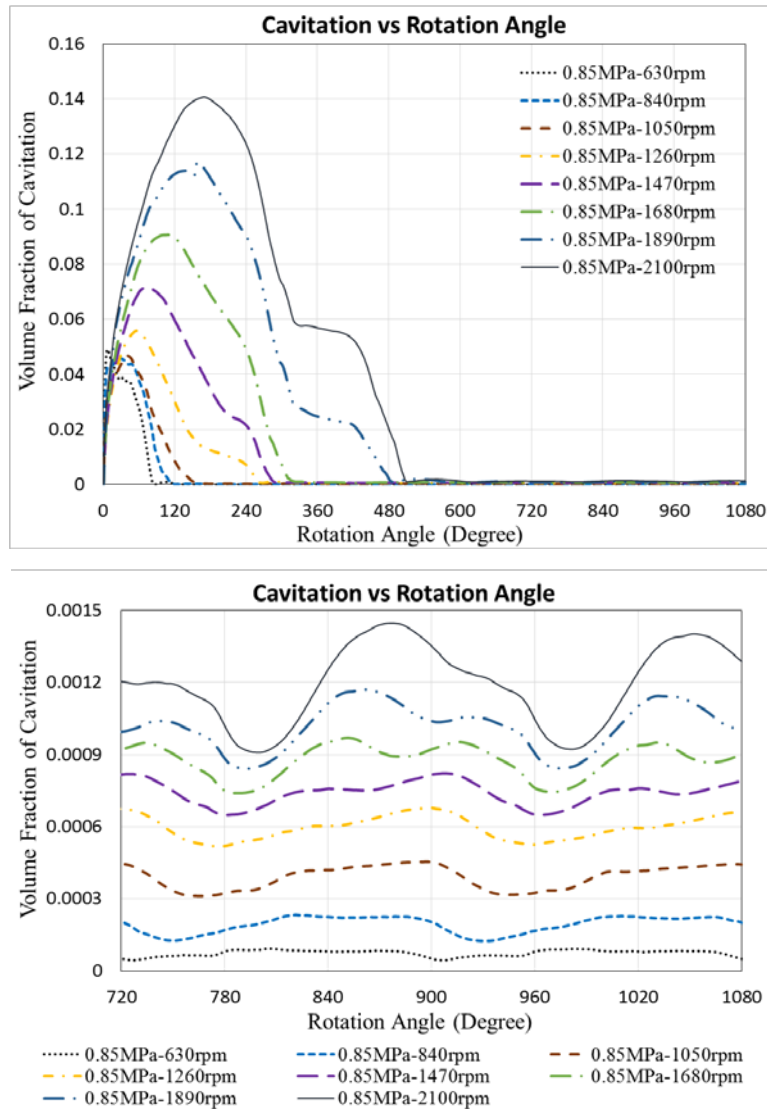


Figure 6 Cavitation changes under different rotation speeds at different rotation angles: (up)0°-1080°; (down)720°-1080°

Figure 7(up) shows the changes of the maximum volume fraction of vapour with the constant rotation speed at different discharge pressures. The peak volume fraction of vapour value slightly reduced with the increase of the discharge pressure, while the frequency remained the same. When the pump reached steady state conditions the amplitude of volume fraction remains higher for higher pressure difference between the suction and discharge pressures as shown in Figure 7(down).

Compared with Figure 6, it can be observed that the effect of the discharge pressure on cavitation is not as significant as in the case of increased rotation speed.

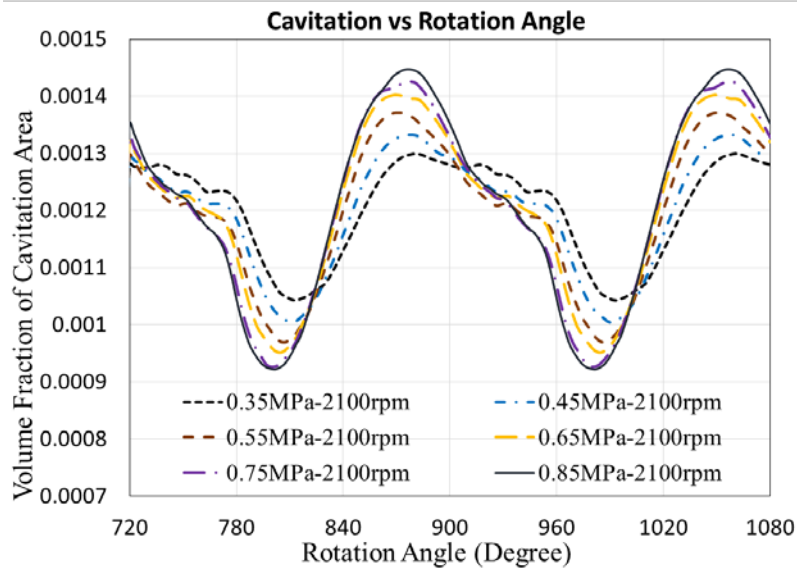
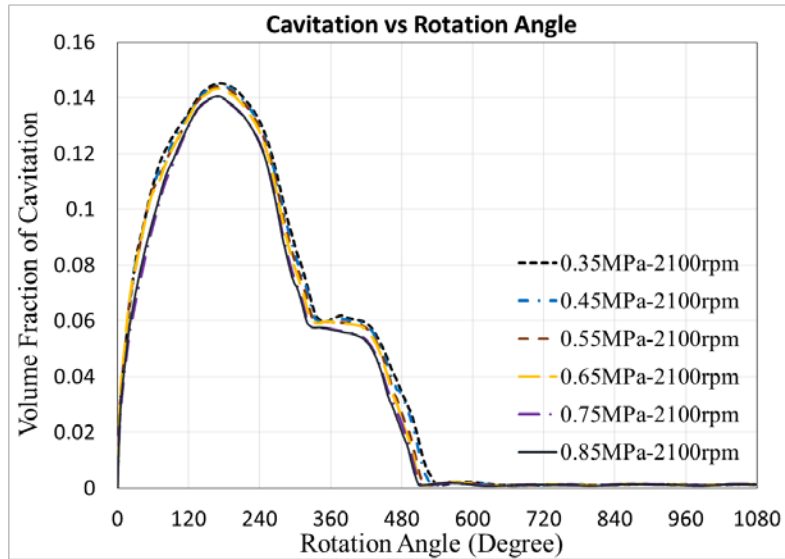


Figure 7 Cavitation changes under different discharge pressure at different rotation angles: (up)0°-1080°; (down)720°-1080°

Figure 8 shows the location of the cavitation area at different rotor angle when the screw pump reaches a relatively stable state at 2100rpm and 0.85MPa. The increased volume fraction of vapour is mainly located in the radial and inter-lobe clearances near the suction port, and its value changes periodically with the rotation of the rotors.

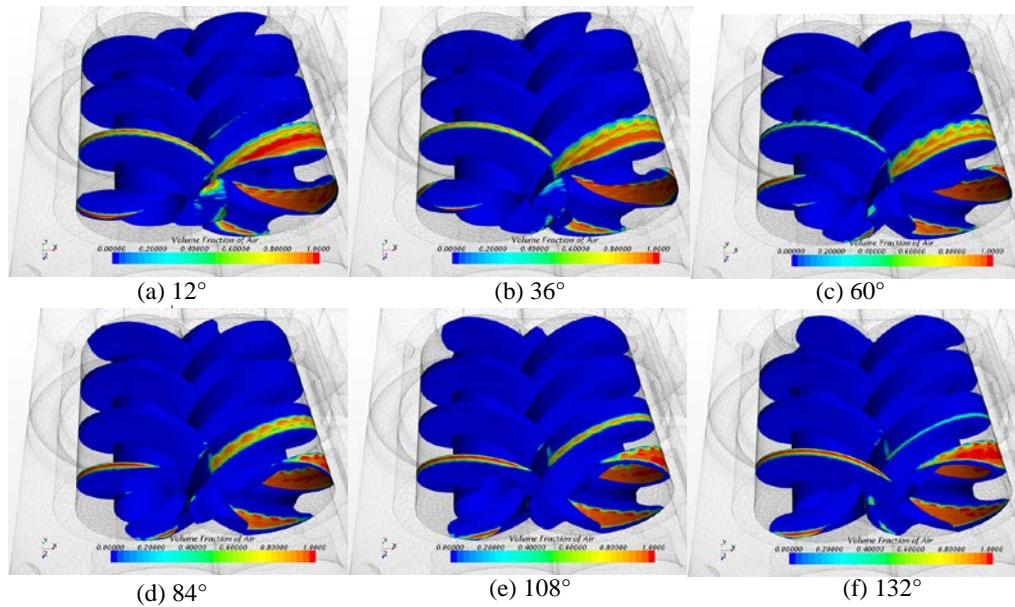


Figure 8 Cavitation distribution at 2100rpm and 0.85MPa under different rotation angle

Figure 9 shows the variation of cavitation area at different rotor angle when the screw pump reaches a relatively stable state at 630rpm and 0.85MPa. The area where fluid cavitates is the same as for the higher speed but its amplitude is much smaller especially on the female rotor. Compared with values in Figure 8 for speed of 2100 rpm, it can be concluded that the cavitation weakens with the decrease of rotation speed.

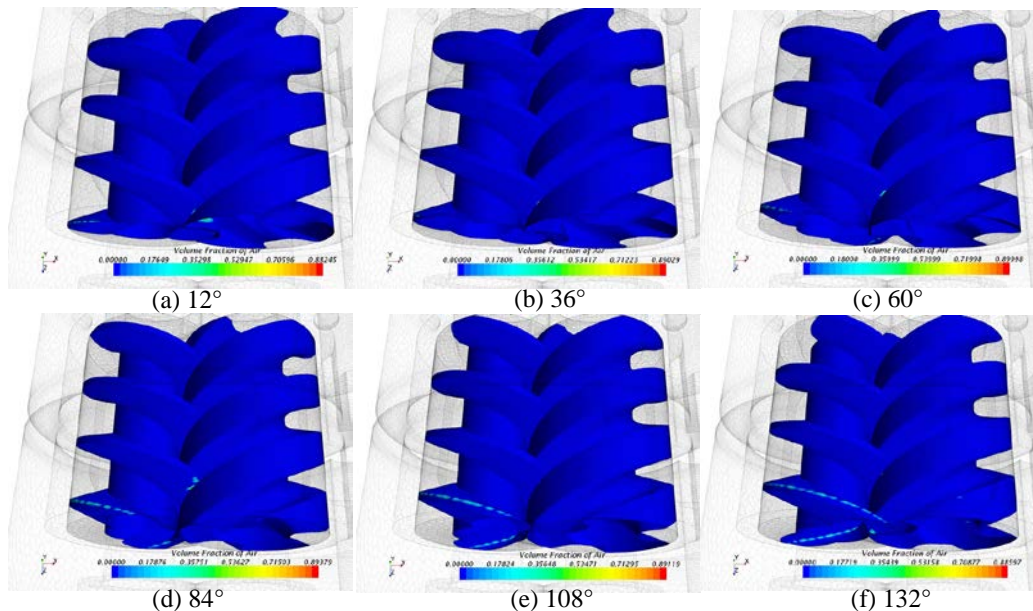


Figure 9 Cavitation distribution at 630rpm and 0.85MPa under different rotation angle

To investigate what will happen at much higher speeds, a calculation is performed for 4 times the maximum speed of the liquid pump, in this case 8400 rpm. In such case, cavitation is not limited just to the clearance area, it extends to the entire chamber and also will spread to other chambers in the axial direction from the suction. This is shown in Figure 10 for same angles of rotation as in previous figures. It would take much longer for cavitation to reduce. The mean value of the volume fraction of vapour and its amplitude would both increase compared to lower

speeds shown in previous figures.

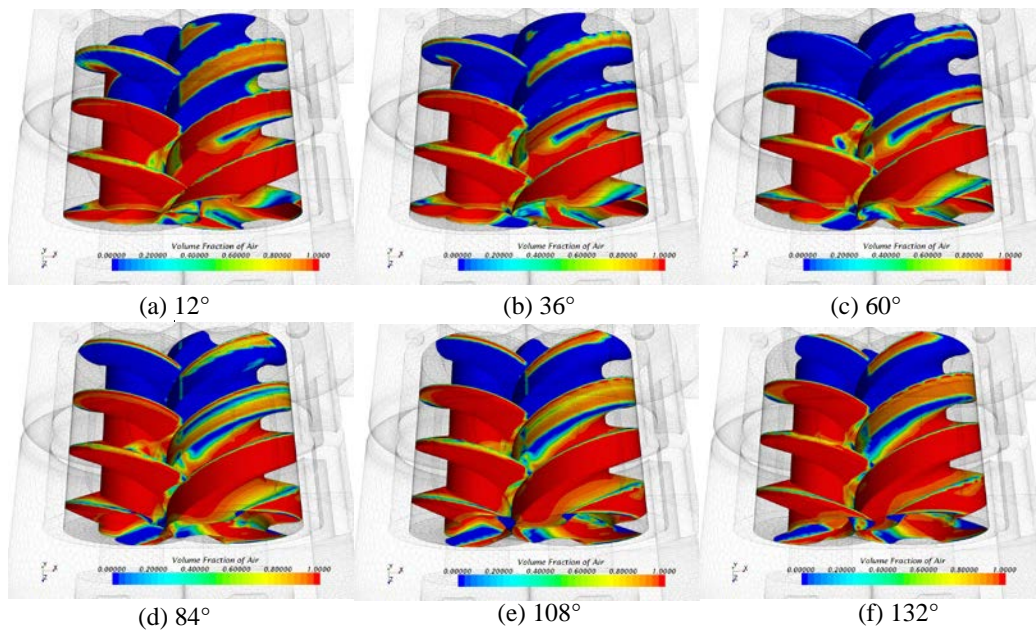


Figure 10 Cavitation distribution at 8400rpm and 0.85MPa under different rotation angles

## 4.2 Mass Flow Rate

In order to investigate effects of cavitation on the flow through the pump, two separate calculations were performed at 2100rpm and 0.85MPa discharge pressure, one without cavitation and another which includes modelling of the cavitation.

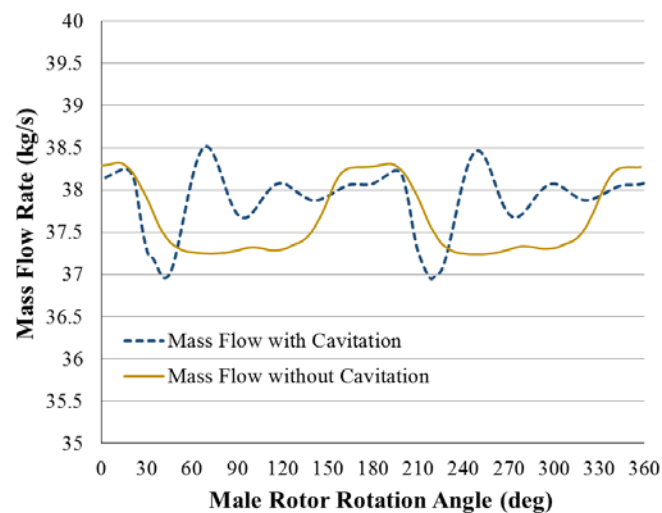


Figure 11 Mass flow rate with and without cavitation under different rotation angle

Figure 11 shows the calculated instantaneous mass flow rate of the screw pump with and without cavitation at 2100rpm and 0.85MPa. It can be seen from the comparison that the mass flow pulsations with cavitation included in prediction model are larger than that without cavitation, the fluctuation amplitude without cavitation is 0.62kg/s while under cavitation it is

1.03kg/s. The averaged mass flow rate under cavitation is similar to that without cavitation.

### 4.3 Rotor Torque

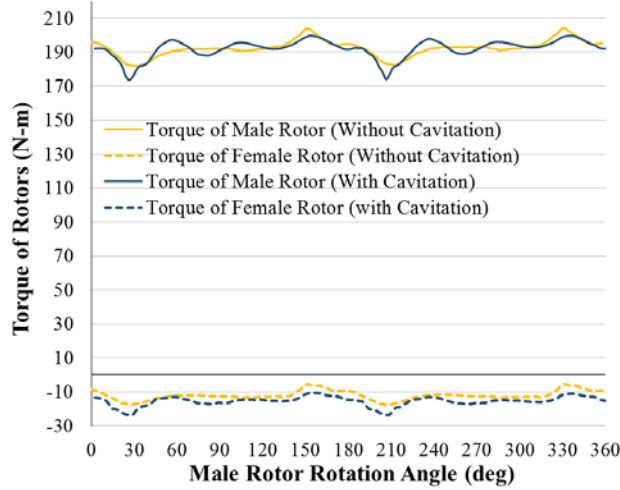


Figure 12 Rotor torque with and without cavitation under different rotation angle

Figure 12 shows the rotor torque of screw pump with and without cavitation at 2100rpm and 0.85MPa. The periods of torque fluctuations with and without cavitation are the same. Cavitation brings a slightly increased amplitude of torque value. For the male rotor, the fluctuation of torque without cavitation is 11.83N-m, while which increases to 18.43N-m when with cavitation. The averaged torque of male rotor with and without cavitation are the same, while cavitation causes an increase of 3.17N-m which is 26.04% in averaged female rotor torque.

## 5. Comparison with experiment and discussion

Performance prediction of the liquid pump analysed in this paper was validated for a single phase calculation in previous publication by the authors [35]. It included validation of internal and integral parameters as well as the grid independency study and comparison of different turbulence modes. This paper extends on [35] to include cavitation without introducing any additional phenomena. The working medium used in the experiment is CD40 lubricating oil. The density is 889kg/m<sup>3</sup> and the dynamic viscosity is 5.25×10<sup>-2</sup> Pa·S. The temperature of oil is 50 to 70°C. The nominal interlobe clearance (between two rotors) is 0.12 mm, the nominal radial clearance (between rotor and casing) is 0.24 mm.

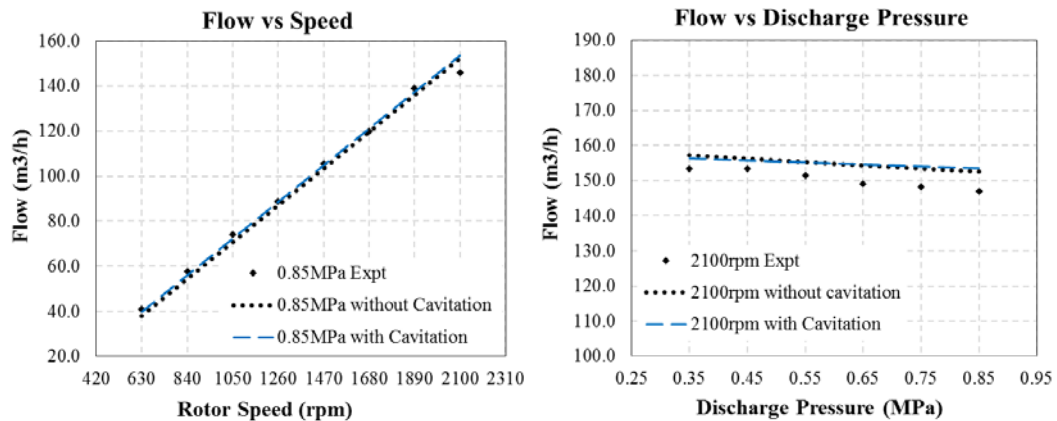


Figure 13 Mass flow rate: (left) variable rotational speed; (right) variable discharge pressure

Figure 13(left) shows the mass flow rate obtained with and without cavitation modelling for of rotational speeds between 630 and 2100 rpm and the constant discharge pressure 0.85MPa. By comparison, it can be found that with cavitation the mass flow rate is 4.90% higher than that without cavitation.

From the distribution of cavitation in Figure 8, it can be seen that under a relatively low rotation speed cavitation mainly appeared in clearance area. Clearance cavitation leads to a decrease of mass flow rate through clearances, which means smaller leakage rate. It is observed by analysing modelling results that forming of the vapour in clearances effects sealing and it brings a slightly increased volumetric efficiency of a screw pump. The mechanism of cavitation in clearances will be further analysed and discussed in Chapter 6 .

Figure 13(right) shows the mass flow rate of cavitation and non-cavitation condition with the variation of discharge pressure and (under constant rotation speed 2100rpm). It can be found that the mass flow rates of both are very close. With the increase of discharge pressure, the mass flow rate under cavitation gradually exceeds that without cavitation in a small degree.

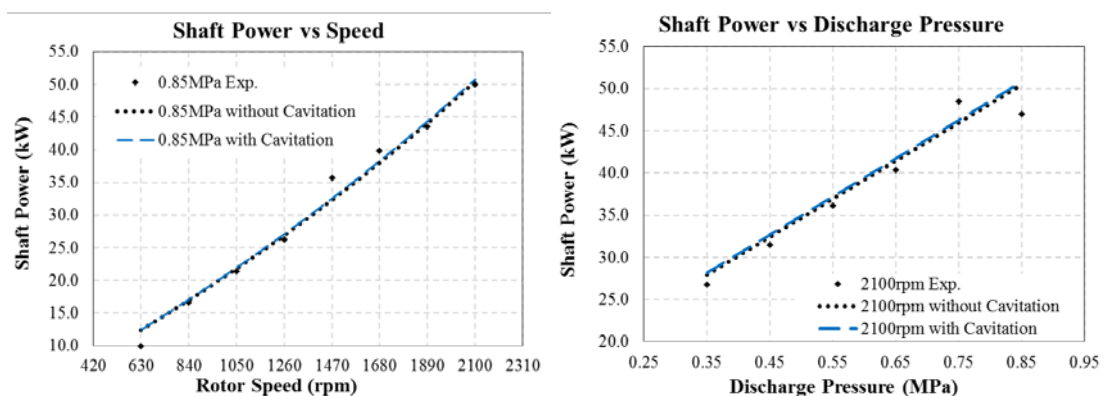


Figure 14 Shaft power: (left) variable rotational speed; (right) variable discharge pressure

Figure 14(left, right) shows the shaft power of screw pump under cavitation and non-cavitation with the variation of rotation speed and discharge pressure. It can be found that cavitation and non-cavitation have a very close shaft power while cavitation brings a slightly increase of 1.21% in shaft power. The main reason caused higher power consumption is that cavitation influenced the pressure distribution in chamber and brought fluctuation and increase in rotor torque.

## 6. Mechanism of Clearance Cavitation in Twin-screw Pumps

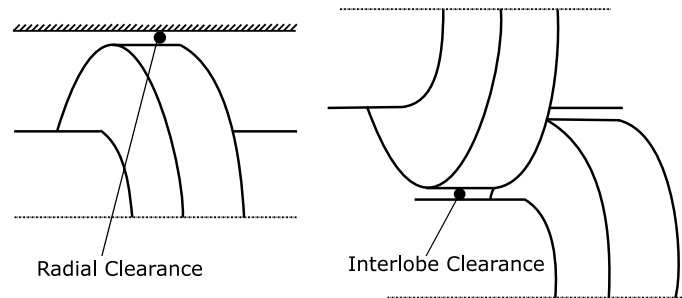


Figure 15 Radial clearance and inter-lobe clearance in screw pump

The characteristics of flow field in clearances play an important role in determining the performance (such as leakage rate, volumetric efficiency) of rotary screw machines [42][43]. When designing screw rotors, two types of clearances need to be considered, radial clearance and inter-lobe clearance (Figure 15).

From the full 3D CFD modelling of screw pump, it is found that after reaching a relatively stable state the cavitation is mainly distributed in clearances when the rotation speed is not too high. According to the Couette-Poiseuille flow model [44], the flow field of clearances can be simplified, and the approximate distribution of pressure and velocity can be obtained. The mechanism of clearance cavitation can be deduced and simplified as shown in Figure 16.

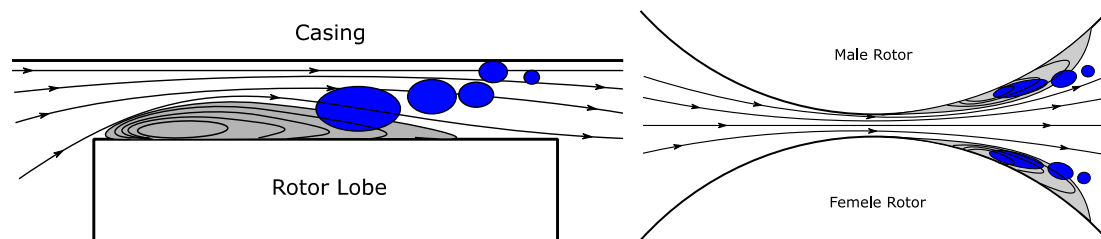
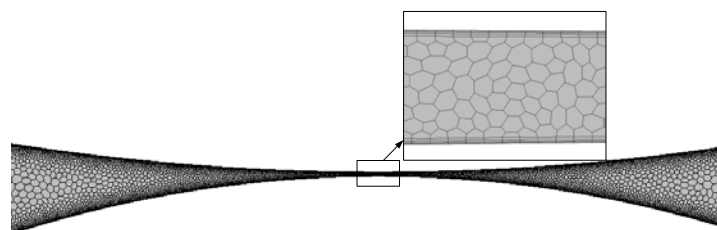


Figure 16 Schematic diagram of clearance cavitation

### 6.1 2-D Numerical Model Setup and Simulation

In order to reveal and understand more deeply the formation mechanism of clearance cavitation in screw pumps and its influence in leakage rate, 2-D numerical models of radial and inter-lobe clearances flow has been built. Based on polygonal mesh and prism boundary layer mesh, the numerical 2-D mesh was generated as Figure 17. There are 4 prism layers for the moving boundaries. A numerical mesh of 91082 cells was used for interlobe clearance, while a numerical mesh of 52454 cells was used for radial clearance.



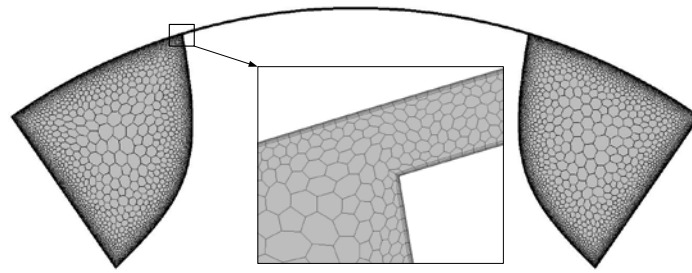


Figure 17 Grid generation for inter-lobe clearance (up) and radial clearance (down)

Pressure inlet and pressure outlet are used as boundary conditions. The pressure values are set according to the pressure gradients that obtained by results of full 3-D CFD simulation of screw pump. In order to simulate the real working condition of clearances, moving boundaries are applied in the walls that represent the surfaces of rotors and the velocities of moving boundaries are chosen based on the rotation speed of rotors. Reynolds Stress Turbulence model was applied in the calculation. By comparing the mass flow rate through clearances under cavitation and non-cavitation, the influence of clearance cavitation on leakage rate of screw pump can be obtained.

## 6.2 Discussion and Analysis

Figure 18 reflects the distribution of cavitation in clearance area. According to calculation results, it can be found that cavitation area will be increased with the increase of rotation speed and pressure difference.

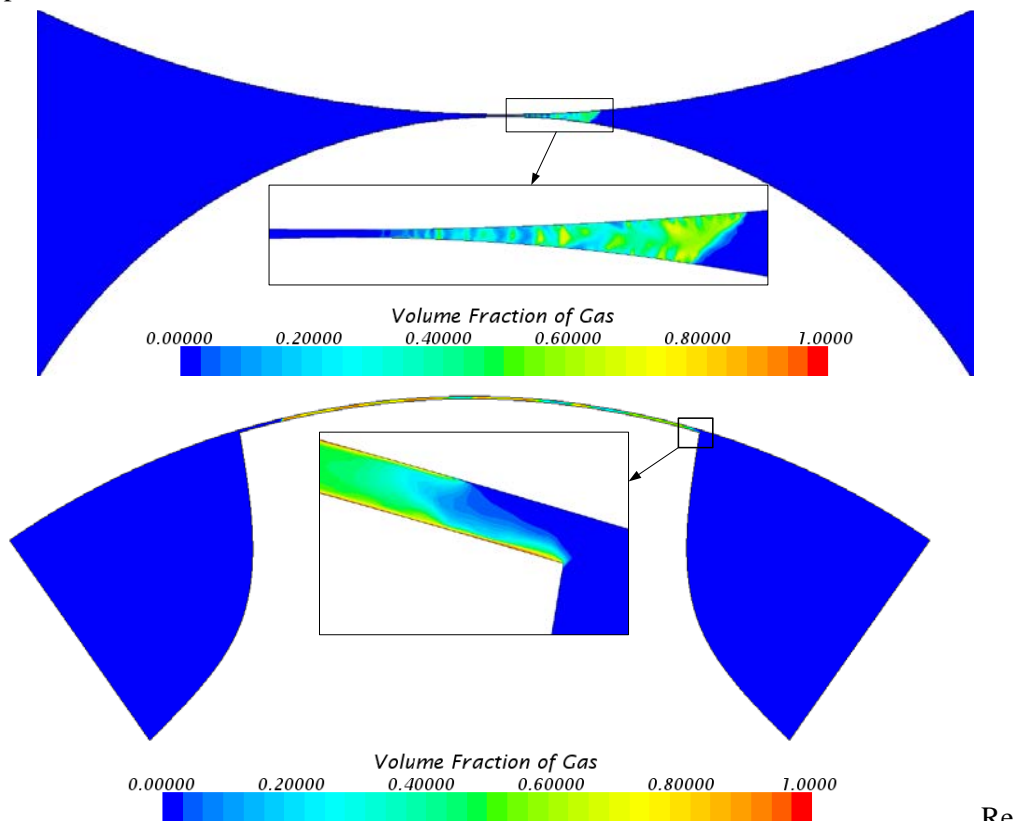


Figure 18 Cavitation distribution in inter-lobe clearance (up) and radial clearance (down)

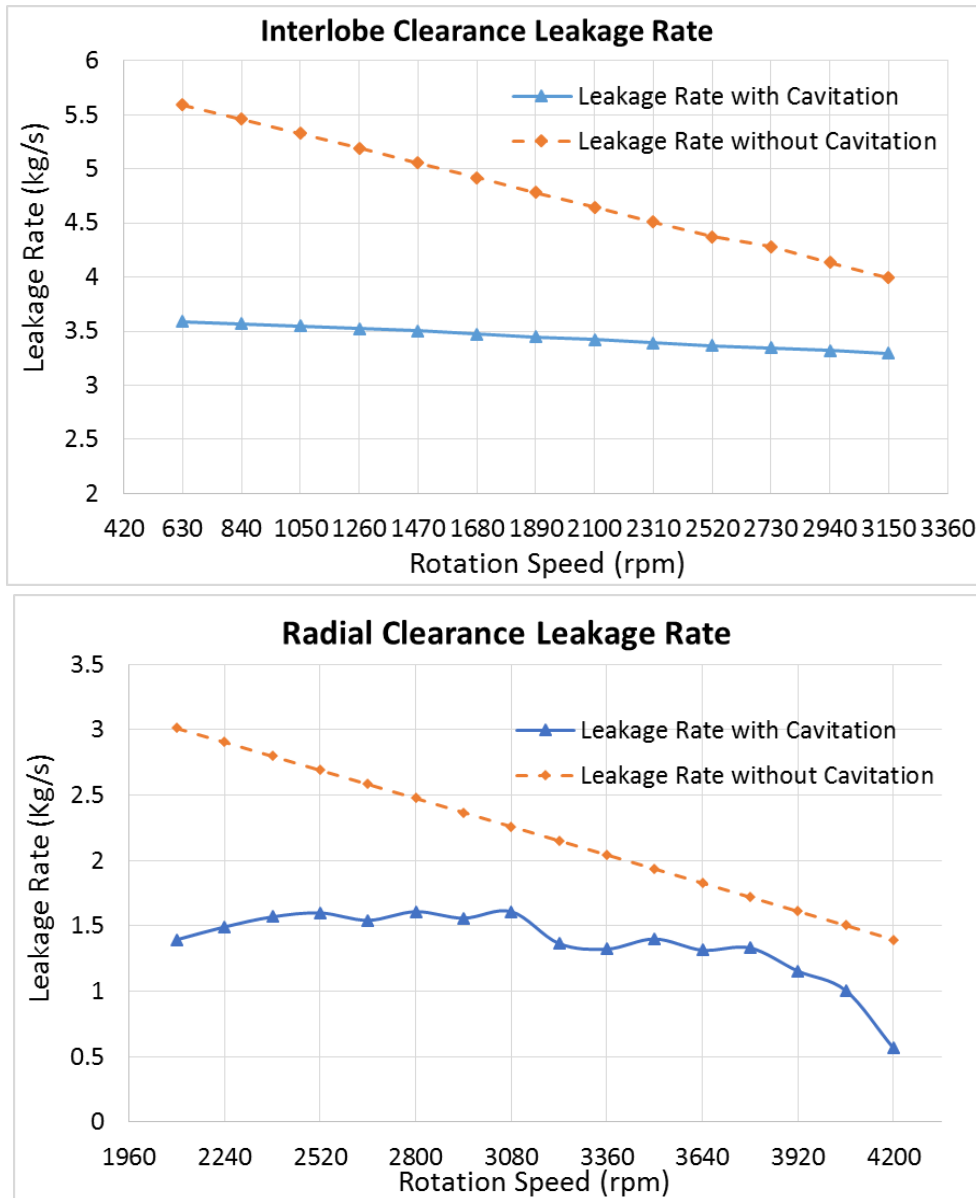


Figure 19 leakage rate through clearances with and without cavitation: (up) inter-lobe clearance; (down) radial clearance

Figure 19 shows the mass flow rate of cavitation under cavitation and non-cavitation through clearances. It can be found that the mass flow rate under cavitation is smaller than that without cavitation, and with the increase of cavitation, the difference between this two becomes more obvious.

From the calculation above, the relationship between clearance cavitation and leakage rate can be obtained. When cavitation appears in clearances, the mass flow rate through clearances will be reduced, namely, the leakage rate of screw pump will be reduced. Accordingly, the volumetric efficiency will be increased slightly. With the further increasing of rotation speed, the cavitation area will be expanded to the chamber between rotor lobes (Figure 10), large amounts of bubbles will be formed and the interaction will decrease the real mass flow rate of screw pump, which means a decrease of volumetric efficiency. The qualitative relationship

between cavitation and volumetric efficiency can be described as in Figure 20.

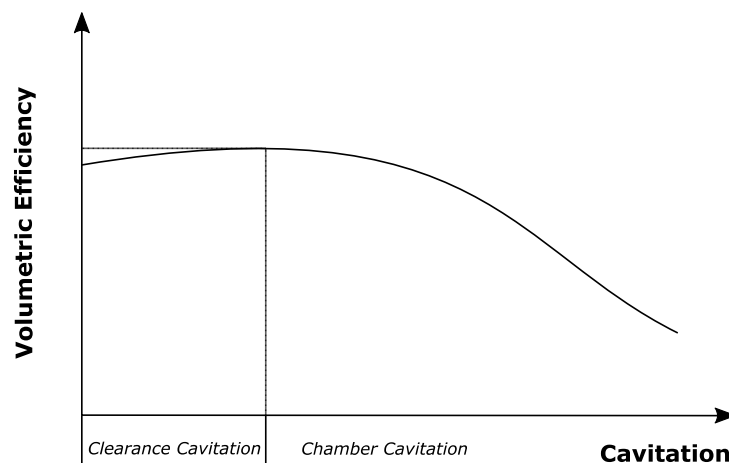


Figure 20 Relationship between cavitation and volumetric efficiency

## 7. Conclusions

A full 3-D CFD simulation of twin-screw pump has been carried out using structured moving numerical mesh with the conformal interface between the rotor domains. The cavitation intensity and distribution area were predicted based on the combination of VOF method and the Sauer-Scherr model. Through analysis and discussion, it can be concluded as follows:

- (1) If it appears, the cavitation will mainly happen in the area close to the suction port and will be distributed in the outward surfaces of rotors and clearances when the rotation speed is not too high. With the increase of rotation speeds beyond the current limit of pumps, the cavitation area will expand to the whole chamber along the rotor from suction to discharge.
- (2) The increase of rotation speed will enlarge the intensity of cavitation observably in screw pump. The decrease of the discharge pressure at constant speed of rotation will slightly increase the cavitation which can be neglected.
- (3) The cavitation in screw pumps has many influence on the pump performance, which is manifested in larger pressure impact in screw rotors, increase of rotor torque and mass flowrate pulsation and larger power consumption.
- (4) Clearance cavitation can reduce the leakage rate through clearances, which result in a slightly increased volumetric efficiency. With the expansion of cavitation area, massive bubbles will be generated in pump chamber which leads to a markedly decline of volumetric efficiency.

The study of use of CFD for screw pumps provides better understanding of the internal flow field and cavitation characteristics, which provides a good basis for the next-step research on multiphase screw pump under different volume fraction of gas (VFG).

**Acknowledgments:** This research was supported by the National Natural Science Foundation of China [grant number 51575069], State Key Program of National Natural Science of China [grant number 51635003], Program of International S&T Corporation [grant number 2014DFA73030], and China Scholarship Council [grant number 201406050094]. The project was performed at City University of

London.

## References

- [1] Luca d'Agostino, Maria Salvetti, CISM International Centre for Mechanical Sciences: Fluid Dynamics of Cavitation and Cavitating Turbopumps, Udine: Springer-Verlag Wien, 2007. ISBN 978-3-211-76668-2.
- [2] Ruschel Andrej, Fluiddynamische Effekte in Schraubenspindelpumpen bei der Multiphasenförderung (Fluiddynamic effects in screw pumps at multiphase operation), Shaker Verlag GmbH, PhD thesis, Erlangen-Nürnberg University, 2014.
- [3] Brennen Christopher, Cavitation and Bubble Dynamics, New York: Oxford University Press, 1995. ISBN 0-19-509409-3.
- [4] O. A. ПЫЖ, Marine Screw Pump (in Chinese), Hefei: Hefei General Machinery Research Institute, 1969.
- [5] Futian Li, Screw Pump, Beijing: China Machine Press, 2010. ISBN 9787111297949.
- [6] Feng Cao, Yueyuan Peng, Ziwen Xing, Pengcheng Shu. Thermodynamic Performance Simulation of a Twin-Screw Multiphase Pump, Proceedings of the IMechE, Part E:Journal of Process Mechanical Engineering, pp. 157-162, 2001.
- [7] Qian Tang, Yuanxun Zhang, Screw Optimization for Performance Enhancement of a Twin-Screw Pump, Proceedings of the IMechE, Part E:Journal of Process Mechanical Engineering, vol. 228, no. 1, pp. 73-84, 2014.
- [8] Jing Wei, Research on Rotor Profiles Design Method and Numerical Simulation for Twin-screw Kneader, Journal of Mechanical Engineering (Chinese Edition), vol. 49, no. 3, pp. 63-73, 2013.
- [9] D Mewes, G Aleksieva, A Scharf, A Luke, Modelling Twin-Screw Multiphase Pumps – A Realistic Approach to Determine the Entire Performance Behaviour, 2nd International EMBT Conference, Hannover, 2008.
- [10] Abhay Patil. Performance Evaluation and CFD Simulation of Multiphase Twin-Screw Pumps, PhD Thesis, Texas A&M University, Texas, 2013.
- [11] Evan Chen, Wet-Gas Compression in Twin-Screw Multiphase Pumps, MS Thesis, Texas A&M University, Texas, 2006.
- [12] Rübiger K. Edmund, Fluid Dynamic and Thermodynamic Behaviour of Multiphase Screw Pumps Handling Gas-Liquid Mixtures with Very High Gas Volume Fractions, PhD Thesis, University of Glamorgan, Treforest, 2009.
- [13] Dzhanakmedov A. K., Investigations of the destructive effect of two-phase liquid on screw pump lip seals, Journal of Friction and Wear, vol. 29, no. 4, p. 310–313, 2008.
- [14] Wentao Qu, Zhangshi Xu, Hong Zhang. Petroleum Drilling Techniques, "Theoretical study on leakage model of submersible twin-screw pump, vol. 35, no. 6, pp. 76-78, 2007.
- [15] Ahmed Kovacevic, Nikola Stosic, Ian K Smith. Three Dimensional Numerical Analysis of Screw Compressor Performance, Journal of Computational Methods in Sciences and Engineering, vol. 3, no. 2, pp. 259- 284, 2003.
- [16] Nikola Stosic, Ian K Smith, Ahmed Kovacevic. Screw Compressors Mathematical Modelling and Performance Calculation, Berlin Heidelberg New York: Springer, 2005. ISBN-10 3-540-24275-9.
- [17] Ahmed Kovacevic, Nikola Stosic, Ian K Smith. Screw Compressors Three Dimensional

Computational Fluid Dynamics and Solid Fluid Interaction, Berlin Heidelberg New York: Springer, 2006. ISBN-10 3-540-36302-5.

- [18] David del Campo, R Castilla, GA Raush, PJ Gamez-Montero, E Codina. Pressure effects on the performance of external gear pumps under cavitation, Proceedings of the IMechE, Part C: Journal of Mechanical Engineering Science, vol. 228, no. 16, pp. 2925-2937, 2014.
- [19] Washio Seiichi, Recent Developments in Cavitation Mechanisms: A Guide for Scientists and Engineers, Cambridge: Elsevier Woodhead Publishing, 2014. ISBN 978-1-78242-175-7.
- [20] Manolis Gavaises, Fabio Villa, Phoevos Koukouvinis, Marco Marengo, Jean-Pierre Franc. Visualisation and les simulation of cavitation cloud formation and collapse in an axisymmetric geometry, International Journal of Multiphase Flow, vol. 68, pp. 14-26, 2015.
- [21] Mitroglou N, Lorenzi M, Santini M, Gavaises M, Assanis D., Application of cone-beam micro-CT on high-speed Diesel flows and quantitative cavitation measurements, in Journal of Physics: Conference Series, 2015.
- [22] Singhal AK, Athavale M, Li HY., Mathematical basis and validation of the full cavitation model, Journal of Fluids Engineering, vol. 124, no. 3, p. 617–624, 2002.
- [23] Philip Zwart, Andrew Gerber, Thabet Belamri. A two-phase flow model for predicting cavitation dynamics, in ICMF 2004 International Conference on Multiphase Flow, Yokohama, 2004.
- [24] Robert F. Kunz, David A. Boger, David R. Stinebring, Thomas S. Chyczewski, Jules W. Lindau, A preconditioned Navier–Stokes method for two-phase flows with application to cavitation prediction, Computers & Fluids, vol. 29, no. 8, p. 849–875, 2000.
- [25] Günter H. Schnerr, Jürgen Sauer. Physical and numerical modeling of unsteady cavitation dynamics, in Fourth International Conference on Multiphase Flow, New Orleans, 2001.
- [26] Jürgen Sauer, Günter H. Schnerr. Unsteady cavitating flow: a new cavitation model based on a modified front capturing method and bubble dynamics, in 2000 ASME Fluids Engineering Summer Conference, Boston.
- [27] Weixing Yuan, Jürgen Sauer, Günter H. Schnerr. Modeling and computation of unsteady cavitation flows in injection nozzles, Mécanique & Industries, vol. 2, no. 5, pp. 383-394, 2001.
- [28] Mireia Altimira, Laszlo Fuchs. Numerical investigation of throttle flow under cavitating conditions, International Journal of Multiphase Flow, vol. 75, p. 124–136, 2015.
- [29] Desheng Zhang, Lei Shi, Weidong Shi, Ruijie Zhao, etc. Numerical analysis of unsteady tip leakage vortex cavitation cloud and unstable suction-side-perpendicular cavitating vortices in an axial flow pump, International Journal of Multiphase Flow, vol. 77, p. 244–259, 2015.
- [30] Yingyuan Liu, Leqin Wang, Zuchao Zhu. Numerical study on flow characteristics of rotor pumps including cavitation, Proceedings of the IMechE, Part C: Journal of Mechanical Engineering Science, vol. 229, no. 14, p. 2626–2638, 2015.
- [31] David del. Campo, Analysis of the suction chamber of external gear pumps and their influence on cavitation and volumetric efficiency, Open Access, PhD thesis, Universitat Politècnica de Catalunya, 2012.
- [32] A King, R Plant, A Kovacevic. Improved design of gear pump porting through CFD simulation, in International conference on compressors and their systems, Oxford, 2009.

- [33] Sham Rane, Ahmed Kovacevic, Nikola Stosic. Analytical Grid Generation for accurate representation of clearances in CFD for Screw Machines, in 9th International Conference on Compressors and their Systems, London, 2015.
- [34] STAR-CCM+ Version 9.06.009 Tutorial Guide.
- [35] Di Yan, Ahmed Kovacevic, Qian Tang, Sham Rane, Wenhua Zhang, Numerical Modelling of Twin-screw Pumps Based on Computational Fluid Dynamics, Proceedings of IMechE, Part C: Journal of Mechanical Engineering Science, vol. 0, no. 0, pp. 1-18, 2016.
- [36] Ahmed Kovacevic, Di Yan, Qian Tang, Sham Rane. Numerical Investigation of Twin-Screw Pump by Use of CFD, Proceeding of 13<sup>th</sup> Fluid Machinery Congress, Hague, 3-4 October 2016. ISBN 978-0-9956263-0-0
- [37] C.W Hirt, B.D Nichols, Volume of fluid (VOF) method for the dynamics of free boundaries, Journal of Computational Physics, vol. 39, no. 1, pp. 201-225, 1981.
- [38] I. Demirdžić, S. Muzaferija, Numerical Method for Coupled Fluid Flow, Heat Transfer and Stress Analysis Using Unstructured Moving Mesh with Cells of Arbitrary Topology, Computer Methods in Applied Mechanics and Engineering , vol. 125, no. 1-4, pp. 235-255, 1995.
- [39] Joel H. Ferziger, Milovan Peric, Computational Methods for Fluid Dynamics, 3rd Edition ed., Berlin Heidelberg: Springer-Verlag, 2002. ISBN 3-540-42074-6.
- [40] P. S. Epstein, M. S. Plesset. On the Stability of Gas Bubbles in Liquid-Gas Solutions, vol. 18, no. 11, pp. 1505-1509, 1950.
- [41] Sham Rane, Grid Generation and CFD analysis of variable Geometry Screw Machines, PhD thesis, City University London, London, 2015.
- [42] Z H Fong, F C Huang. Evaluating the interlobe clearance and determining the sizes and shapes of all the leakage paths for twin-screw vacuum pump, Proceedings of the IMechE, Part C:Journal of Mechanical Engineering Science, vol. 220, no. 4, pp. 499-506, 2006.
- [43] Jan Vimmr, Modelling of complex clearance flow in screw-type machines, Mathematics and Computers in Simulation, vol. 76, no. 1-3, p. 229–236, 2007.
- [44] Gräßer Melanie, Brümmer Andreas. An analytic model of the incompressible one-phase clearance flow in liquid injected screw expanders, in 9th International Conference on Screw Machines, Düsseldorf, 2014.

<b>Nomenclature</b>			
$\alpha_v$	vapour volume fraction	$f$	function of enveloping
$R_0$	initial average seed radius of bubble	$R$	seed radius
$n_0$	an average seed density of bubble	$i$	one phase in the fluid
$V_v$	volume of vapour	$V_l$	volume of liquid
$P_B$	pressure at bubble boundary	$P_\infty$	ambient cell pressure
$\Delta t$	time-step	$\phi$	angle of rotation
$DPTS$	the degree of rotation per time step	$u$	velocity
$RPM$	rotation speed of male rotor	$\omega$	angular velocity of rotor
$S_{\alpha_i}$	the source of the phase $i$	$\rho$	density
$\Omega$	control volume	$\Gamma$	diffusion coefficient
$\mathbf{n}$	cell face normal vector	$\mathbf{v}$	fluid velocity

$S$	cell surface	$\mathbf{v}_b$	surface velocity
$q_{\phi s}$	flux source	$q_{\phi v}$	volume source